

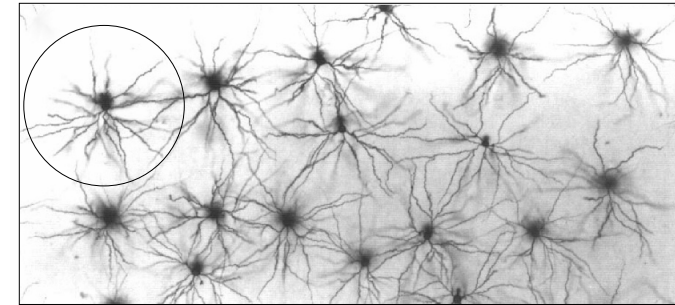
Modeling the Visual System

Dr. James A. Bednar

jbednar@inf.ed.ac.uk

http://homepages.inf.ed.ac.uk/jbednar

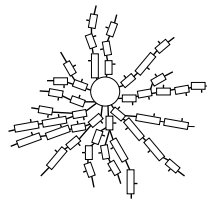
Sample network to model



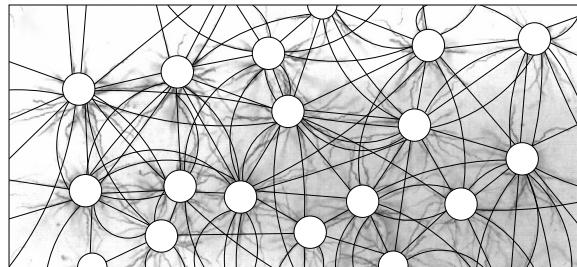
CMVC figure 3.1a

Tangential section with a small subset of neurons labeled
Where do we begin?

Modeling approaches



Compartmental neuron model



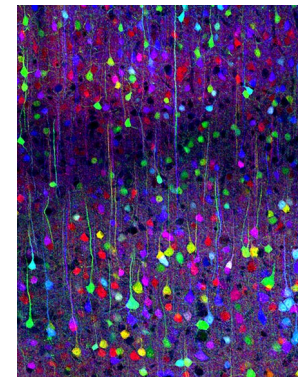
Integrate-and-fire / firing-rate model of the network

CMVC figure 3.1b,e

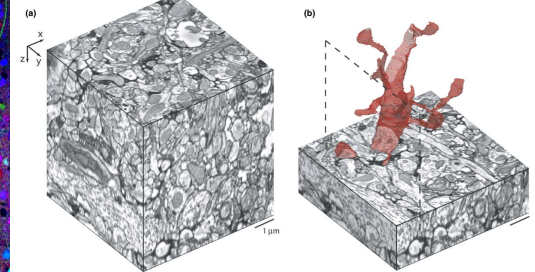
One approach: model single cells extremely well
Our approach: many, many simple single-cell models

Dense connectivity

(Livet et al. 2007)



Brainbow mouse cortex



Electron microscopy of rat cortex

(Briggman & Denk 2006)

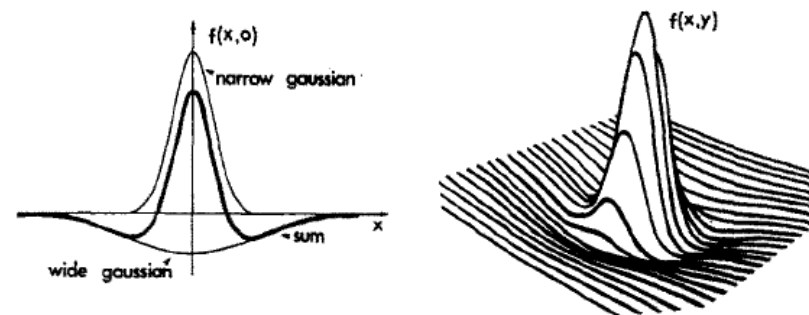
Remember that the actual network is far denser than in the previous slides, with many opportunities for contact between neurons and neurites.

Levels of explanation

There are many ways to explain the electrophysiological properties (the behavior) of V1 neurons:

1. **Phenomenological:** Mathematical fit to behavior – a good model iff there is a good fit to adults
2. **Mechanistic:** good if a good type 1 model *and* also consistent with circuits or other mechanisms in adults
3. **Developmental:** good if a good type 2 model *and* explains how it comes about, consistent with known data
4. **Normative:** good if a good type 1, 2, or 3 model *and* explains why the behavior is useful or appropriate

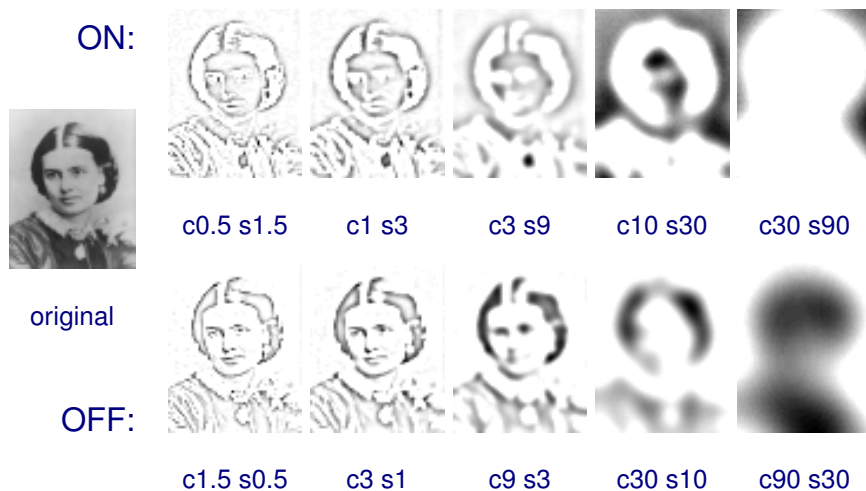
Adult retina and LGN cell models



(Rodieck 1965)

- Standard model of adult RGC or LGN cell activity: Difference of Gaussians weight matrix
- Firing rate: dot product of weight and input matrices
- Can be tuned for quantitative match to firing rate
- Can add temporal component (transient+sustained)

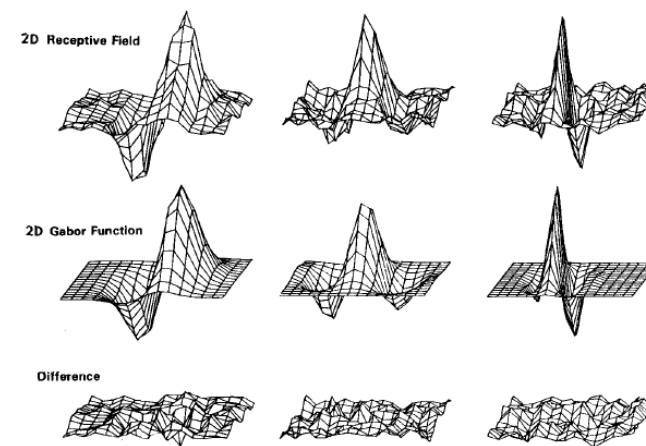
Effect of DoG



Each DoG, if convolved with the image, performs edge enhancement at a certain size scale (spatial frequency

band)

Adult V1 cell model: Gabor

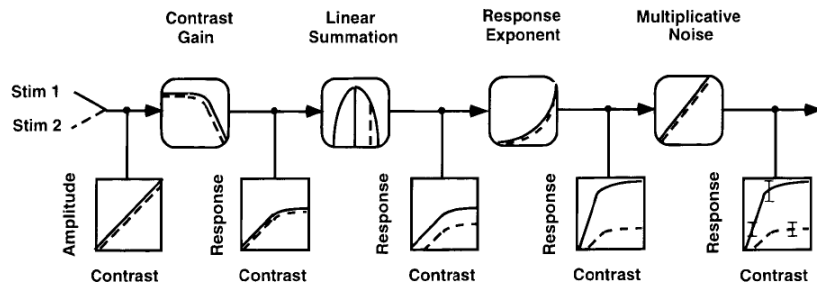


(Adult cat; Daugman 1988)

Standard model of adult V1 simple cell spatial preferences:
Gabor (Gaussian times sine grating) (Daugman 1980)

Adult V1 cell model: CGE

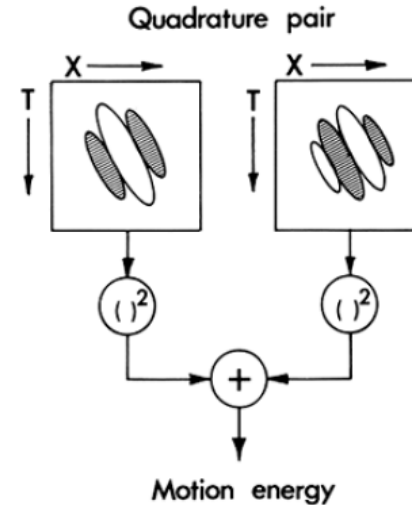
Contrast-Gain Exponent (CGE) Model



(Geisler & Albrecht 1997)

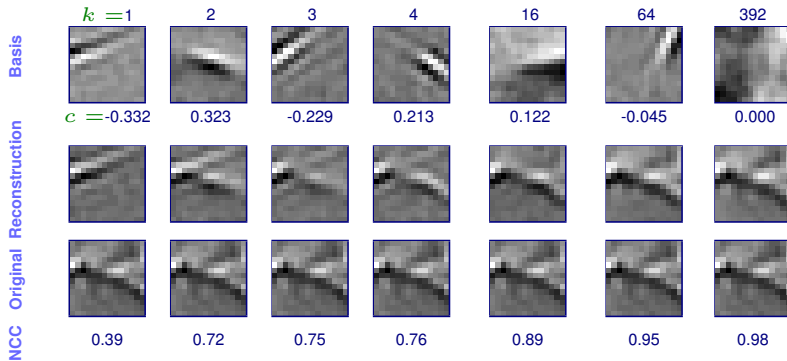
- Gabor model fits spatial preferences
- Simple response function: dot product
- To match observations: need to add numerous nonlinearities
- Examples: CGE model (Geisler & Albrecht 1997); LN model

Adult V1 cell model: Energy

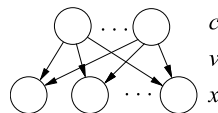


- Spatiotemporal energy: Standard model of complex direction cell (Adelson & Bergen 1985)
- Combines inputs from a quadrature pair (two simple cell motion models out of phase)
- Achieves phase invariance, direction selectivity

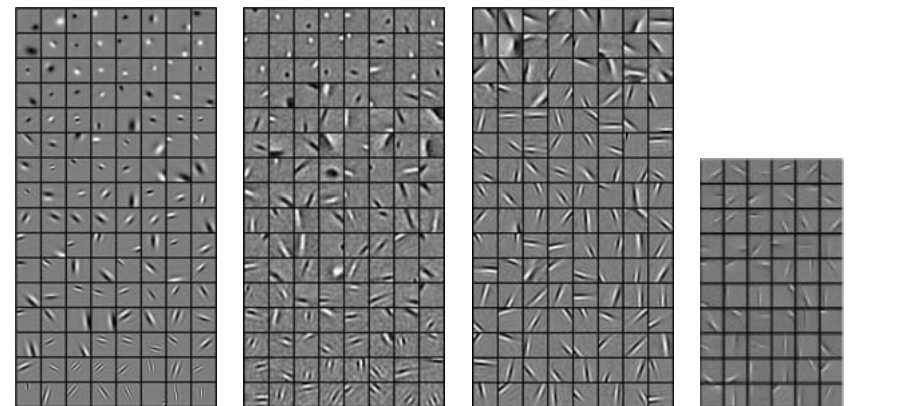
V1 cells as a sparse basis set



One way to think about these cells: Basis vectors (here from Olshausen & Field 1996) supporting reconstruction of the inputs, in a generative model $x \approx \sum_i c_i v_i$:



Macaque and model V1 cells



Macaque (Ringach 2002)

SSC (Rehn & Sommer 2007)

SparseNet (Olshausen & Field 1996)

ICA (van Hateren et al. 1998)

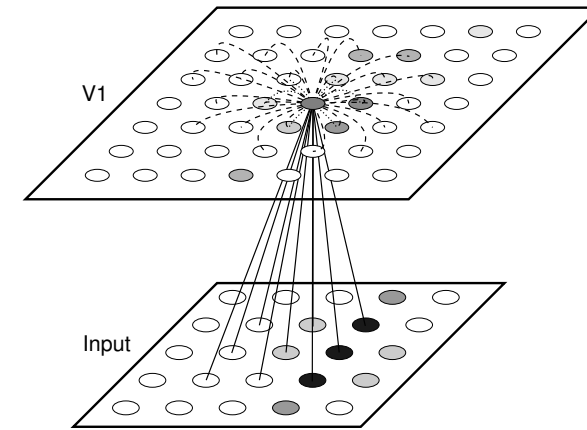
Reproducing full range of RFs may require special sparseness constraints (SSC)

Retina/LGN development models

- Retinal wave generation
(e.g. Feller et al. 1997; Godfrey & Swindale 2007; Hennig et al. 2009)
- RGC development based on retinal waves
(e.g. Eglén & Willshaw 2002)
- Retinogeniculate pathway based on retinal waves
(e.g. Eglén 1999; Haith 1998)
- Initial topography: Eph and Ephrin gradient models
(e.g. Willshaw 2006)

Because of the wealth of data from the retina, such models can now become quite detailed.

Our focus: Cortical map models



Basic architecture: input surface mapped to cortical surface + some form of lateral interaction

Kohonen SOM: Feedforward

Popular computationally tractable map model (Kohonen 1982)

Feedforward activity of unit (i, j) :

$$\eta_{ij} = \|\vec{V} - \vec{W}_{ij}\| \quad (1)$$

(distance between input vector \vec{V} and weight vector \vec{W})

Not particularly biologically plausible, but easy to compute, widely implemented, and has some nice properties.

Note: Activation function is not typically a dot product; the CMVC book is confusing about that.

Kohonen SOM: Lateral

Abstract model of lateral interactions:

- Pick winner (r, s)
- Assign it activity η_{\max}
- Assume that activity of unit (i, j) can be described by a neighborhood function, such as a Gaussian:

$$h_{rs,ij} = \eta_{\max} \exp \left(-\frac{(r-i)^2 + (s-j)^2}{\sigma_h^2} \right), \quad (2)$$

Models lateral interactions that depend only on distance from a single winning unit.

Kohonen SOM: Learning

Inspired by basic Hebbian rule (Hebb 1949):

$$w' = w + \alpha \eta \chi \quad (3)$$

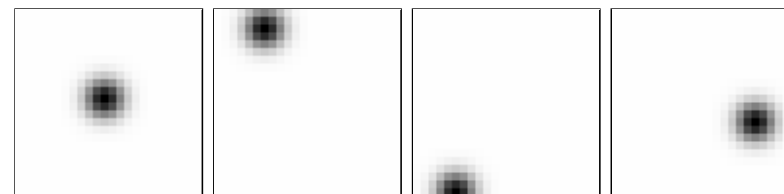
where the weight increases in proportion to the product of the input and output activities.

In SOM, the weight vector is shifted toward the input vector based on the Euclidean difference:

$$w'_{k,ij} = w_{k,ij} + \alpha(\chi_k - w_{k,ij})h_{rs,ij} \quad (4)$$

Hebb-like, but depending on distance from winning unit

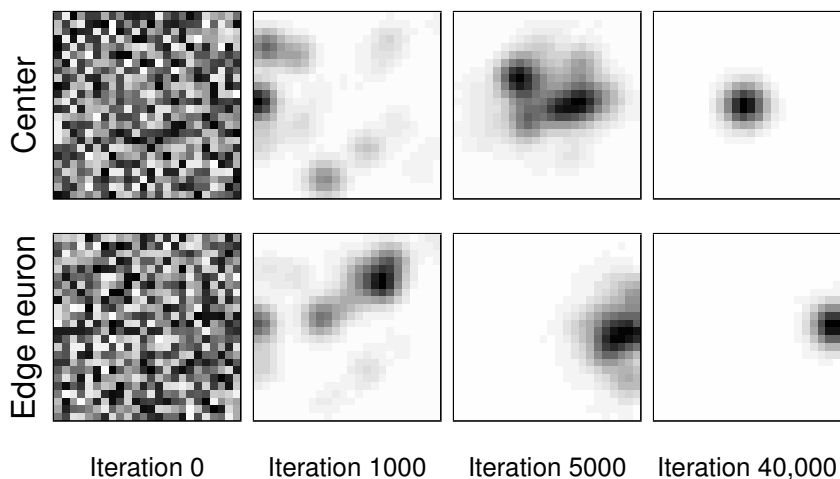
SOM example: Input



CMVC figure 3.4

- SOM will be trained with unoriented Gaussian activity patterns
- Random (x, y) positions anywhere on retina
- 576-dimensional input, but the x and y locations are the only source of variance

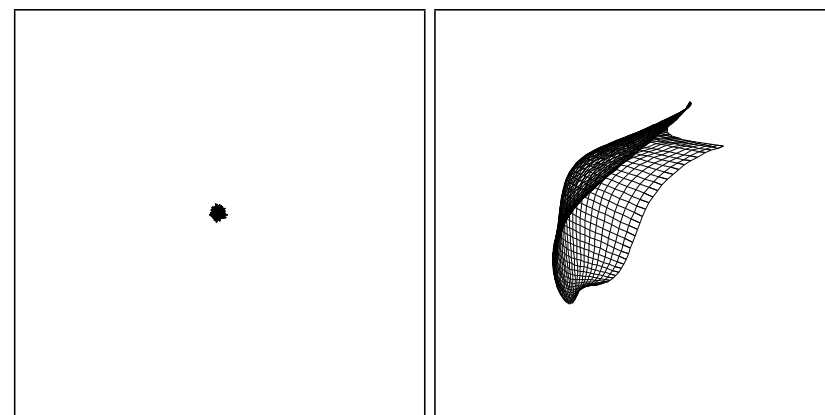
SOM: Weight vector self-org



CMVC figure 3.5

Combination of input patterns; eventually settles to an exemplar

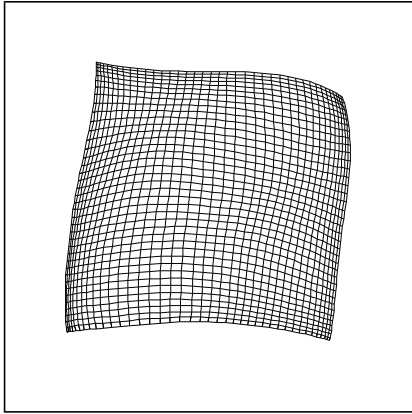
SOM: Retinotopy self-org



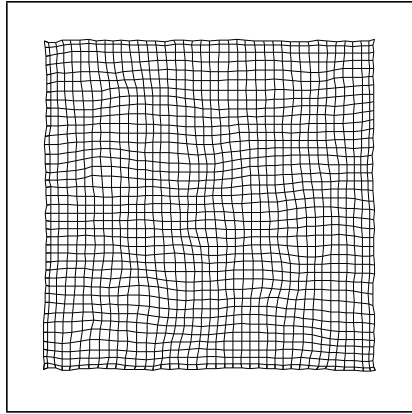
CMVC figure 3.6a-b

- Initially bunched (all average to zero)
- Unfolds as neurons differentiate

SOM: Retinotopy self-org



Iteration 5000: Expanding

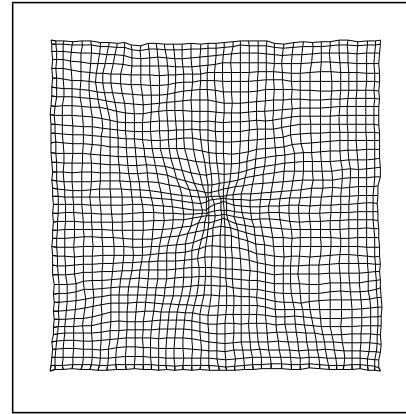


Iteration 40,000: Final

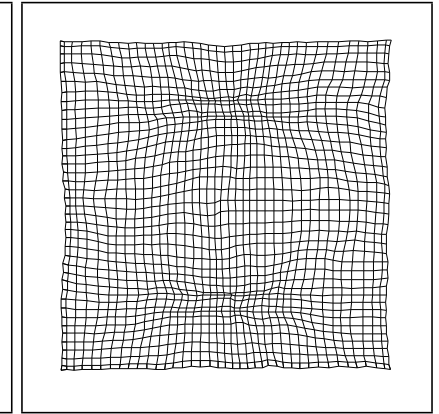
Expands to cover usable portion of input space.

CMVC figure 3.6c-d

Magnification of dense input areas



Gaussian distribution

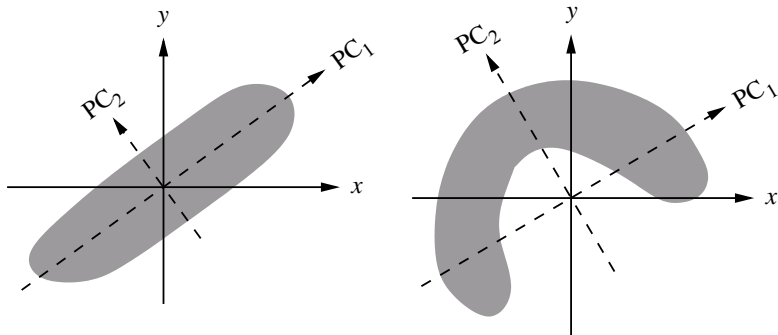


Two long Gaussians

Density of units receiving input from a particular region depends on input pattern statistics

CMVC figure 3.7

Principal components of data distributions



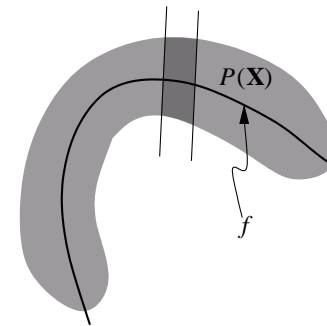
(a) Linear distribution

(b) Nonlinear distribution

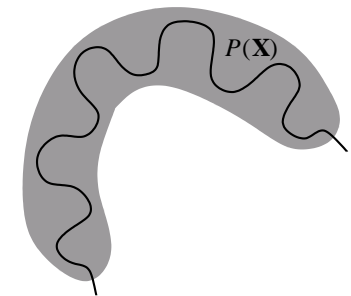
CMVC figure 3.8

PCA: linear approximation, good for linear data

Nonlinear distributions: principal curves, folding



Principal curve



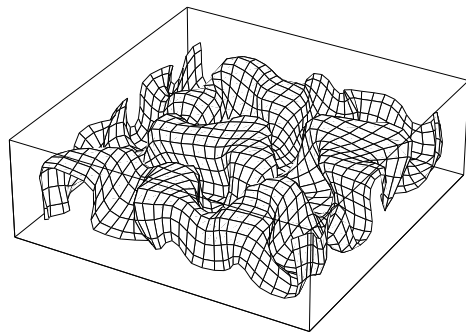
Folded curve

Generalization of idea of PCA to pick best-fit curve(s)

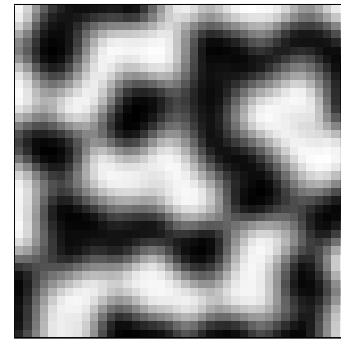
Multiple possible curves

CMVC figure 3.9

Three-dimensional model of ocular dominance



Representing the third dimension by folding

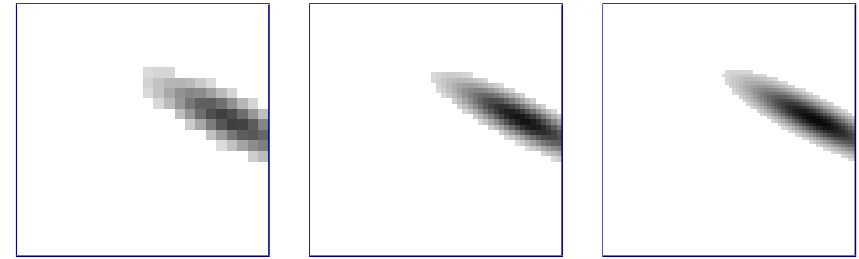


Visualization of ocular dominance

CMVC figure 3.10

Feature maps: Discrete approximations to principal surfaces?

Role of density of input sheet



- Gaussian inputs are nearly band-limited (since Fourier transform is also Gaussian)
- Density of input sampling unimportant, if it's greater than 2X highest frequency in input (Nyquist theorem)

Role of density of SOM sheet

SOM sheet acts as a discrete approximation to a two-dimensional surface.

How many units are needed for the SOM depends on how nonlinear the input distribution is — a smoothly varying input distribution requires fewer units to represent the shape.

Only loosely related to the input density — input density limits how quickly the input varies across space, but only for wideband stimuli.

Other relevant models

ICA Independent Component Analysis yields realistic RFs (Bell & Sejnowski 1997); also can be applied to maps (Hyvärinen & Hoyer 2001).

InfoMax Information maximization can lead to RFs (Linsker 1986b,c) and basic maps (Kozloski et al. 2007; Linsker 1986a)

Elastic net Achieving good coverage and continuity leads to realistic feature maps (Carreira-Perpiñán et al. 2005; Goodhill & Cimponeriu 2000)

This course focuses on mechanistic circuit models, not normative models (ICA, Infomax, PCA, principal surfaces) or feature space models (elastic net), both of which are hard to relate directly to the underlying biological systems.

Summary

- Basic intro to visual modeling
- Adult models are well established, but vision-specific
- SOM: maps multiple dimensions down to two
- Feature maps: Principal surfaces?

References

- Adelson, E. H., & Bergen, J. R. (1985). Spatiotemporal energy models for the perception of motion. *Journal of the Optical Society of America A*, *2*, 284–299.
- Bell, A. J., & Sejnowski, T. J. (1997). The “independent components” of natural scenes are edge filters. *Vision Research*, *37*, 3327.
- Briggman, K. L., & Denk, W. (2006). Towards neural circuit reconstruction with volume electron microscopy techniques. *Current Opinion in Neurobiology*, *16* (5), 562–570.
- Carreira-Perpiñán, M. A., Lister, R. J., & Goodhill, G. J. (2005). A computational model for the development of multiple maps in primary visual cortex. *Cerebral Cortex*, *15* (8), 1222–1233.

Daugman, J. G. (1980). Two-dimensional spectral analysis of cortical receptive field profiles. *Vision Research*, *20*, 847–856.

Daugman, J. G. (1988). Complete discrete 2-D Gabor transforms by neural networks for image analysis and compression. *IEEE Transactions on Acoustics, Speech, and Signal Processing*, *36* (7).

Eglen, S. J. (1999). The role of retinal waves and synaptic normalization in retinogeniculate development. *Philosophical Transactions of the Royal Society of London Series B*, *354* (1382), 497–506.

Eglen, S. J., & Willshaw, D. J. (2002). Influence of cell fate mechanisms upon retinal mosaic formation: A modelling study. *Development*, *129* (23), 5399–5408.

Feller, M. B., Butts, D. A., Aaron, H. L., Rokhsar, D. S., & Shatz, C. J. (1997). Dynamic processes shape spatiotemporal properties of retinal waves. *Neuron*, *19*, 293–306.

Geisler, W. S., & Albrecht, D. G. (1997). Visual cortex neurons in monkeys and cats: Detection, discrimination, and identification. *Visual Neuroscience*, *14* (5), 897–919.

Godfrey, K. B., & Swindale, N. V. (2007). Retinal wave behavior through activity-dependent refractory periods. *PLoS Computational Biology*, *3* (11), e245.

Goodhill, G. J., & Cimponeriu, A. (2000). Analysis of the elastic net model applied to the formation of ocular dominance and orientation columns. *Network: Computation in Neural Systems*, *11*, 153–168.

Haith, G. L. (1998). *Modeling Activity-Dependent Development in the Retinogeniculate Projection*. Doctoral Dissertation, Department of Psychology, Stanford University, Palo Alto, CA.

Hebb, D. O. (1949). *The Organization of Behavior: A Neuropsychological Theory*. Hoboken, NJ: Wiley.

Hennig, M. H., Adams, C., Willshaw, D., & Sernagor, E. (2009). Early-stage retinal waves arise close to a critical state between local and global functional network connectivity. *The Journal of Neuroscience*, *29*, 1077–1086.

Hyvärinen, A., & Hoyer, P. O. (2001). A two-layer sparse coding model learns simple and complex cell receptive fields and topography from natural images. *Vision Research*, *41* (18), 2413–2423.

Kohonen, T. (1982). Self-organized formation of topologically correct feature maps. *Biological Cybernetics*, *43*, 59–69.

Kozloski, J., Cecchi, G., Peck, C., & Rao, A. R. (2007). Topographic infomax in a neural multigrid. In Liu, D. e. a. (Ed.), *Advances in Neural Networks – ISSN 2007* (Lecture Notes in Computer Science4492, pp. 500–509). Berlin: Springer.

Linsker, R. (1986a). From basic network principles to neural architecture: Emergence of orientation columns. *Proceedings of the National Academy of Sciences, USA*, *83*, 8779–8783.

Linsker, R. (1986b). From basic network principles to neural architecture: Emergence of orientation-selective cells. *Proceedings of the National Academy of Sciences, USA*, *83*, 8390–8394.

Linsker, R. (1986c). From basic network principles to neural architecture: Emergence of spatial-opponent cells. *Proceedings of the National Academy of Sciences, USA*, *83*, 7508–7512.

Livet, J., Weissman, T. A., Kang, H., Draft, R. W., Lu, J., Bennis, R. A., Sanes, J. R., & Lichtman, J. W. (2007). Transgenic strategies for combinatorial expression of fluorescent proteins in the nervous system. *Nature*, *450*, 56–62.

Olshausen, B. A., & Field, D. J. (1996). Emergence of simple-cell receptive field properties by learning a sparse code for natural images. *Nature*, *381*, 607–609.

Rehn, M., & Sommer, F. T. (2007). A network that uses few active neurones to code visual input predicts the diverse shapes of cortical receptive fields. *Journal of Computational Neuroscience*, *22* (2), 135–146.

Ringach, D. L. (2002). Spatial structure and symmetry of simple-cell receptive fields in macaque primary visual cortex. *Journal of Neurophysiology*, *88* (1), 455–463.

Rodieck, R. W. (1965). Quantitative analysis of cat retinal ganglion cell response to visual stimuli. *Vision Research*, *5* (11), 583–601.

van Hateren, J. H., & van der Schaaf, A. (1998). Independent component filters of natural images compared with simple cells in primary visual cortex. *Proceedings of the Royal Society London B.*, *265*, 359–366.